Compact triple-mode filter based on quarter-mode substrate integrated waveguide

Jin, Cheng; Shen, Zhongxiang

2014

Jin, C., Shen, Z., Li, R., & Alphones, A. (2014). Compact Circularly Polarized Antenna Based on Quarter-Mode Substrate Integrated Waveguide Sub-Array. IEEE Transactions on Antennas and Propagation, 62(2), 963-967.

https://hdl.handle.net/10356/103922

https://doi.org/10.1109/TMTT.2013.2293128

Compact Triple-Mode Filter Based on Quarter-Mode Substrate Integrated Waveguide

Cheng Jin, *Member, IEEE,* and Zhongxiang Shen, *Senior Member, IEEE*

***Abstract*—An isosceles right triangular waveguide with one electric wall and two magnetic walls is proposed to design a triple-mode filter implemented in substrate integrated waveguide. The complete closed-form modal solutions are presented for both transverse electric and transverse magnetic modes in the isosceles right triangular waveguide. The resonant frequencies of a resonator made of a short isosceles right triangular waveguide can then be calculated. A structure named as quarter-mode substrate integrated waveguide (QMSIW) is introduced to realize the proposed triangular waveguide resonator in a compact and planar form. Simulated electric field distributions of modes excited in the QMSIW are in good agreement with theoretical predictions for the solid waveguide structure, demonstrating the feasibility of QMSIW resonators. Finally, a compact triple-mode filter is designed and fabricated based on the discussed QMSIW. The frequency responses and group delay of the filter are tested, and measured results agree very well with simulated ones. This demonstrates that the proposed QMSIW structure is an excellent candidate for compact triple-mode filters.**

***Index Terms*—Compact bandpass filter, half-mode/quarter-mode substrate integrated waveguide, isosceles right triangular waveguide, triple-mode filter.**

I. Introduction

RECENTLY, the development of compact planar filters has witnessed explosive growth driven by their wide applications in many RF/microwave circuits and systems, such as wireless communications, emerging high-temperature superconducting, and micromachining technologies [**?**], [**?**]. Generally speaking, bandpass filters may be designed using single-, dual- or triple-mode resonators [**?**], [**?**], [**?**], [**?**], [**?**], [**?**]. The tripl-emode resonator possesses three resonances in one resonator, one at the center frequency and the other two near the edges of the passband, resulting in a very good filtering performance and yet retaining its compact size.

A few triple-mode resonators were studied previously in the literature. Most of the published structures are the transmission line based resonators, such as ring resonators [**?**], stub-loaded resonators [**?**], [**?**], stepped impedance resonators (SIR) [**?**], and hybrid microstrip/slotline structures [**?**]. Other types of triple-mode resonators include waveguide cavity resonator [**?**] and multilayer resonator [**?**].These structures exhibit excellent filtering performance. However, the transmission line based resonators generally suffer from higher conductor loss and lower power-handling capability, while the waveguide cavity and multilayer resonators are bulky and difficult to be fabricated and integrated with other circuits. In order to reduce the fabrication complexity, facilitate integration with other planar circuits, and realize broadband passband properties, substrate integrated waveguide (SIW) and half-mode substrate integrated waveguide (HMSIW) have been studied and exploited to design high-performance microwave components in recent years [**?**], [**?**], [**?**], [**?**], [**?**], [**?**], [**?**], [**?**], [**?**]. Most of these resonators operate merely with a single mode within a certain frequency band.

Manuscript received May 6, 2013.

C. Jin is with the Institute of Microelectronics (IME), Singapore 117685 (e-mail: jincheng@ieee.org).

Z. Shen is with the School of Electrical and Electronic Engineering, Nanyang Technological University, Singapore 639798 (e-mail: ezxshen@ntu.edu.sg).

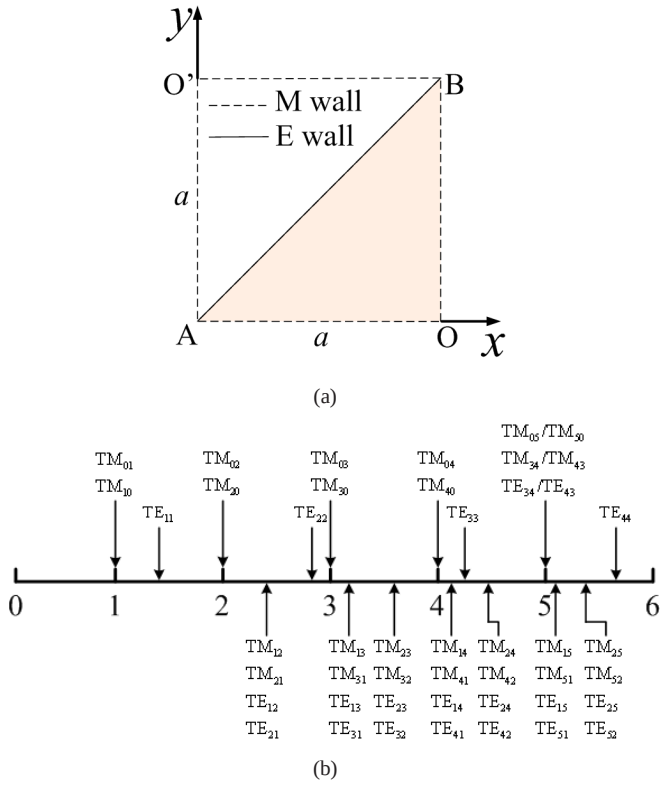

Fig. 1. Cross section and normalized cutoff frequencies of an isosceles right triangular waveguide with two magnetic walls and one electric wall at $y = x$. (a) Geometry. (b) Normalized cutoff frequencies.

An isosceles right triangular resonator with one electric side wall and two magnetic side walls, as shown in Fig. **??** is proposed in this paper. A cavity model is used to analyze the resonator. Closed-form transverse electric (TE) and transverse magnetic (TM) mode solutions of the triangular resonator can be found via superposition of mode solutions for the corresponding square waveguide with magnetic walls [**?**]. Analytical expressions for both TE and TM modes provide

simple solutions that are ready to evaluate resonant frequencies and electromagnetic field components for all eigen modes in the triangular resonator. Based on the analysis of isosceles right triangular resonator, it is found that the structure is an attractive and promising candidate to design compact triple-mode filters.

In order to realize the resonator with the particular boundary conditions, an isosceles right triangular patch resonator loaded with one array of metallic via holes along the hypotenuse is introduced and named as quarter-mode substrate integrated waveguide (QMSIW). It was demonstrated in [**?**], [**?**] that SIW can be bisected along a fictitious quasi-magnetic wall and the SIW becomes a HMSIW, which almost preserves the field distribution of the original SIW [**?**], [**?**]. It is noted that the HMSIW can be bisected again along the symmetrical plane, and resultantly, a QMSIW is realized. The array of metallic via holes approximates the boundary to the conventional electric wall [**?**], while the other two sides are equivalently regarded as magnetic walls [**?**], [**?**].

The main objective of this paper is to propose and study the isosceles right triangular waveguide resonator with one electric side wall and two magnetic side walls and then to explore a new compact triple-band bandpass filter using the QMSIW approach. In Section II, theoretical solutions of the proposed resonator are derived to show the modal solutions and their field patterns. Section III is concerned with the realization of the resonator and implementation of the QMSIW. After demonstrating the resonant characteristics of the QMSIW, A compact triple-mode filter is finally designed based on it. The frequency responses and group delay of the QMSIW filter are simulated and measured to verify the design concept and to assess its filtering performance.

II. Theoretical Formulation

Fig. **??** shows the cross section of the proposed isosceles right triangular waveguide with one electric wall and two magnetic walls. The magnetic walls are at right-angle sides with $y = 0$ and $x = a$ and the electric wall is along the hypotenuse with $y = x$. Similar to the treatment of a square waveguide [**?**], or a normal triangular waveguide [**?**], [**?**], the electromagnetic fields inside the waveguide can be expanded in terms of TE_{mn} and TM_{mn} modes. To illustrate the proposed isosceles right triangular waveguide, the mode functions and associated eigenvalues will be analytically formulated. The modal functions of such isosceles right triangular waveguide can be constructed by a suitable linear superposition of degenerate modes of a square waveguide with magnetic walls.

A. Square Waveguide with Magnetic Walls

Fig. **??** shows the cross section (OAO'B) of a square waveguide with four magnetic walls. The TE and TM mode functions should satisfy the following boundary conditions

$$\begin{cases} \text{TE}: \ H_x|_{y=0,a}=0, \ H_y|_{x=0,a}=0, \\ \qquad \dfrac{\partial H_z}{\partial x}|_{y=0,a}=0, \ \dfrac{\partial H_z}{\partial y}|_{x=0,a}=0, \\ \text{TM}: \ E_x|_{x=0,a}=0, \ E_y|_{y=0,a}=0, \\ \qquad \dfrac{\partial E_z}{\partial x}|_{x=0,a}=0, \ \dfrac{\partial E_z}{\partial y}|_{y=0,a}=0. \end{cases} \tag{1}$$

By solving the Helmholtz wave equations [**?**], subject to the boundary conditions (**??**), the solutions of H_z and E_z for TE_{mn} and TM_{mn} modes are found

$$\begin{cases} \text{TE}: \ H_z = A_{mn} sin\dfrac{m\pi x}{a} sin\dfrac{n\pi y}{a} e^{-j\beta z} \\ \text{TM}: \ E_z = B_{mn} cos\dfrac{m\pi x}{a} cos\dfrac{n\pi y}{a} e^{-j\beta z}, \end{cases} \tag{2}$$

where A_{mn} and B_{mn} are arbitrary amplitude constants, and β is the propagation constant. The transverse field components can be derived using [**?**]

$$\begin{cases} \text{TE}: \ E_x = -\dfrac{j\omega\mu}{k_c^2}\dfrac{\partial H_z}{\partial y}, \ E_y = \dfrac{j\omega\mu}{k_c^2}\dfrac{\partial H_z}{\partial x}, \ E_z = 0, \\ \qquad H_x = -\dfrac{j\beta}{k_c^2}\dfrac{\partial H_z}{\partial x}, \ H_y = -\dfrac{j\beta}{k_c^2}\dfrac{\partial H_z}{\partial y}, \\ \text{TM}: \ H_x = \dfrac{j\omega\epsilon}{k_c^2}\dfrac{\partial E_z}{\partial y}, \ H_y = -\dfrac{j\omega\epsilon}{k_c^2}\dfrac{\partial E_z}{\partial x}, \ H_z = 0, \\ \qquad E_x = -\dfrac{j\beta}{k_c^2}\dfrac{\partial E_z}{\partial x}, \ E_y = -\dfrac{j\beta}{k_c^2}\dfrac{\partial E_z}{\partial y}, \end{cases} \tag{3}$$

where $\mu = \mu_0\mu_r$, $\epsilon = \epsilon_0\epsilon_r$ are the permeability and permittivity of the material inside the waveguide, respectively. $k_c = \sqrt{k^2 - \beta^2}$ is cutoff wavenumber and $k = \omega\sqrt{\mu\epsilon}$ is the wavenumber of the dielectric material filling the waveguide.

B. Isosceles Right Triangular Waveguide with Two Magnetic Side Walls and One Electric Side Wall

The discussed square waveguide has a series TE_{mn} and TM_{mn} modes with the same critical frequencies. By a proper linear combination of these modes, the mode functions of an isosceles right triangular waveguide can be obtained. Fig. **??** shows the cross section (OAB) of the isosceles right triangular waveguide with two magnetic walls and one electric wall. The TM mode functions meet the boundary conditions

$$\frac{\partial E_z}{\partial y}|_{y=0} = 0, \quad \frac{\partial E_z}{\partial x}|_{x=a} = 0, \quad E_z|_{y=x} = 0, \tag{4}$$

while the TE mode functions satisfy

$$H_z|_{y=0} = 0 \ , H_z|_{x=a} = 0 \ , \frac{\partial H_z}{\partial x} - \frac{\partial H_z}{\partial y}|_{y=x} = 0. \tag{5}$$

The mode function,

$$\varphi_{mn}(x,y) = cos\frac{m\pi x}{a} cos\frac{n\pi y}{a} - cos\frac{n\pi x}{a} cos\frac{m\pi y}{a}, \tag{6}$$

describes a possible TM mode in the square waveguide with magnetic walls. Furthermore, this mode function can satisfy the boundary conditions (**??**) when it is applied to the triangular waveguide shown in Fig. **??**. By inspection, it is obvious

that $E_z|_{y=x} = 0$ is satisfied. To show $\frac{\partial E_z}{\partial y}|_{y=0} = 0$ is valid, consider

$$\begin{aligned}&\frac{\partial \varphi(x,y)}{\partial y}|_{y=0}\\&= \frac{m\pi}{a}cos\frac{n\pi x}{a}sin\frac{m\pi y}{a} - \frac{n\pi}{a}cos\frac{m\pi x}{a}sin\frac{n\pi y}{a}\end{aligned} \tag{7}$$

which is 0 when $y = 0$. However, the linearly independent TM mode function

$$cos\frac{m\pi x}{a}cos\frac{n\pi y}{a} + cos\frac{n\pi x}{a}cos\frac{m\pi y}{a}, \tag{8}$$

does not satisfy the boundary condition at $y = 0$, and therefore does not describe a possible mode in the triangular waveguide. Hence, the mode function (**??**) is the TM mode in the triangular waveguide. It can be readily verified that this mode function satisfies the boundary condition $\frac{\partial E_z}{\partial x}|_{x=a} = 0$ as well. No restriction is placed on the values of m and n except that they must be integers and $m \neq n$.

The transverse field components for the TM$_{mn}$ mode can be computed from (**??**) and (**??**) as

$$\begin{cases} E_x = -\frac{j\beta}{k_c^2}B_{mn}\cdot \\ (-\frac{m\pi}{a}sin\frac{m\pi x}{a}cos\frac{n\pi y}{a} + \frac{n\pi}{a}sin\frac{n\pi x}{a}cos\frac{m\pi y}{a})e^{-j\beta z}, \\ E_y = -\frac{j\beta}{k_c^2}B_{mn}\cdot \\ (-\frac{n\pi}{a}cos\frac{m\pi x}{a}sin\frac{n\pi y}{a} + \frac{m\pi}{a}cos\frac{n\pi x}{a}sin\frac{m\pi y}{a})e^{-j\beta z}, \\ E_z = B_{mn}\cdot \\ \qquad (cos\frac{m\pi x}{a}cos\frac{n\pi y}{a} - cos\frac{n\pi x}{a}cos\frac{m\pi y}{a})e^{-j\beta z}, \end{cases} \tag{9}$$

and

$$\begin{cases} H_x = \frac{j\omega\epsilon}{k_c^2}B_{mn}\cdot \\ (-\frac{n\pi}{a}cos\frac{m\pi x}{a}sin\frac{n\pi y}{a} + \frac{m\pi}{a}cos\frac{n\pi x}{a}sin\frac{m\pi y}{a})e^{-j\beta z}, \\ H_y = -\frac{j\omega\epsilon}{k_c^2}B_{mn}\cdot \\ (-\frac{m\pi}{a}sin\frac{m\pi x}{a}cos\frac{n\pi y}{a} + \frac{n\pi}{a}sin\frac{n\pi x}{a}cos\frac{m\pi y}{a})e^{-j\beta z}, \\ H_z = 0. \end{cases} \tag{10}$$

The mode function

$$\psi_{mn}(x,y) = sin\frac{m\pi x}{a}sin\frac{n\pi y}{a} + sin\frac{n\pi x}{a}sin\frac{m\pi y}{a}, \tag{11}$$

for a TE mode in the square waveguide with magnetic walls, satisfies all boundary conditions (**??**) in the triangular waveguide under consideration only when $m \neq 0$ and $n \neq 0$. Similarly, the linearly independent function

$$sin\frac{m\pi x}{a}sin\frac{n\pi y}{a} - sin\frac{n\pi x}{a}sin\frac{m\pi y}{a} \tag{12}$$

is not suitable. The transverse field components for the TE$_{mn}$ mode can be computed from (**??**) and (**??**) as

$$\begin{cases} E_x = -\frac{j\omega\mu}{k_c^2}A_{mn}\cdot \\ (\frac{n\pi}{a}sin\frac{m\pi x}{a}cos\frac{n\pi y}{a} + \frac{m\pi}{a}sin\frac{n\pi x}{a}cos\frac{m\pi y}{a})e^{-j\beta z}, \\ E_y = \frac{j\omega\mu}{k_c^2}A_{mn}\cdot \\ (\frac{m\pi}{a}cos\frac{m\pi x}{a}sin\frac{n\pi y}{a} + \frac{n\pi}{a}cos\frac{n\pi x}{a}sin\frac{m\pi y}{a})e^{-j\beta z}, \\ E_z = 0, \end{cases} \tag{13}$$

and

$$\begin{cases} H_x = -\frac{j\beta}{k_c^2}A_{mn}\cdot \\ (\frac{m\pi}{a}cos\frac{m\pi x}{a}sin\frac{n\pi y}{a} + \frac{n\pi}{a}cos\frac{n\pi x}{a}sin\frac{m\pi y}{a})e^{-j\beta z}, \\ H_y = -\frac{j\beta}{k_c^2}A_{mn}\cdot \\ (\frac{n\pi}{a}sin\frac{m\pi x}{a}cos\frac{n\pi y}{a} + \frac{m\pi}{a}sin\frac{n\pi x}{a}cos\frac{m\pi y}{a})e^{-j\beta z}, \\ H_z = A_{mn} \\ \qquad (sin\frac{m\pi x}{a}sin\frac{n\pi y}{a} + sin\frac{n\pi x}{a}sin\frac{m\pi y}{a})e^{-j\beta z}. \end{cases} \tag{14}$$

The resonant wavenumbers of the TM$_{mn}$ and TE$_{mn}$ modes for the discussed isosceles right triangular waveguide are

$$k_{cmn} = \frac{\pi}{a}\sqrt{m^2+n^2}, \tag{15}$$

where $m = 0, 1, 2, ...$, $n = 0, 1, 2, ...$ and $m + n \neq 0$. The resonant frequencies of TM$_{mn}$ and TE$_{mn}$ modes are then calculated as the following formula

$$f_{mn} = \frac{1}{2a\sqrt{\mu\epsilon}}\sqrt{m^2+n^2} \tag{16}$$

where $\mu = \mu_0\mu_r$, $\epsilon = \epsilon_0\epsilon_r$ are the permeability and permittivity of the substrate, respectively. The normalized cutoff frequencies for the isosceles right triangular waveguide with two magnetic walls and one electric wall at $y = x$ are shown in Fig. **??**. Furthermore, it should be mentioned that the dominant mode of the isosceles right triangular waveguide is TM$_{01}$/TM$_{10}$ mode and the wavenumber for the dominant mode is $k_{c01} = k_{c10} = \pi/a$. The dominant TE mode is TE$_{11}$ mode, and its cutoff wavenumber is $k_{c11} = \sqrt{2}\pi/a$. Fig. **??** shows the transverse modal field lines for the first ten modes in the triangular waveguide.

III. QMSIW RESONATOR AND TRIPLE-MODE FILTER

The isosceles right triangular waveguide with two magnetic walls and one electric wall discussed in the previous section is artificial because it may not exist in reality. In this section, a new structure named as quarter-mode substrate waveguide guide (QMSIW), as shown in Fig. **??**, is proposed to realize the short waveguide with one electric wall and two magnetic walls. It is well known that an array of metallic via holes with suitable via diameter (d) and spacing (s) between adjacent vias approximates very well the conventional electric boundary.

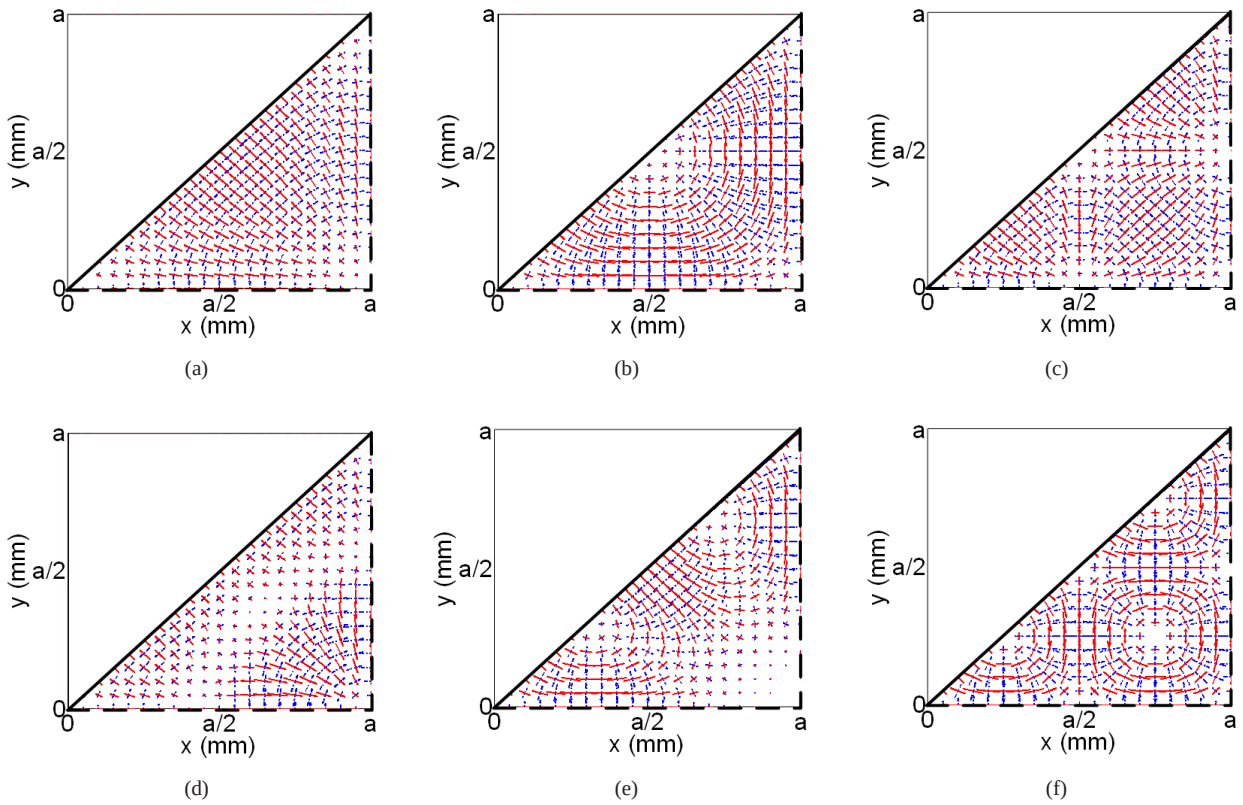

Fig. 2. Transverse modal field distribution for an isosceles right triangular waveguide with two magnetic walls and one electric wall. Red line: electric field. Blue line: magnetic field. (a) TM_{10}/TM_{01}. (b) TE_{11}. (c) TM_{20}/TM_{02}. (d) TM_{12}/TM_{21}. (e) TE_{12}/TE_{21}. (f) TE_{22}.

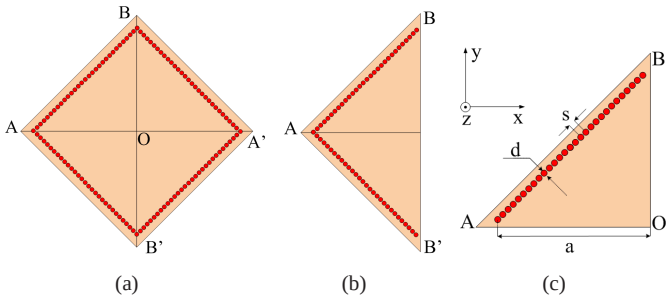

Fig. 3. The process of the evolution of the QMSIW. (a) The square SIW resonator. (b) HMSIW resonator. (c) QMSIW resonator.

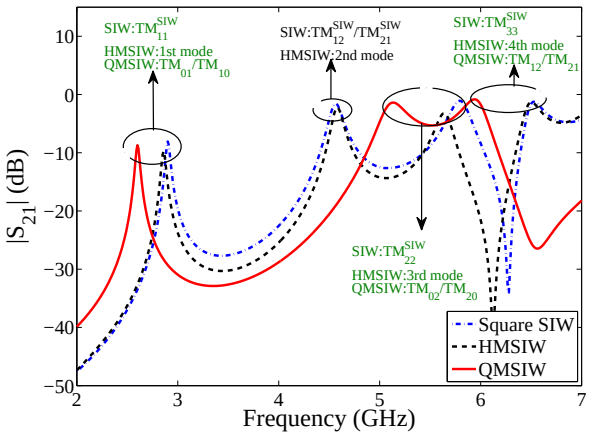

Fig. 4. Simulated transmission coefficients against frequency of the square SIW, HMSIW and QMSIW resonators.

A. QMSIW Resonators

The QMSIW is realized by bisecting the substrate integrated waveguide (SIW) twice along the fictitious magnetic wall. Fig. **??** shows the evolution process of the proposed QMSIW. The electric fields in a square SIW resonator are symmetrical at the center plane along the y-direction. Due to the large SIW width to height ratio, the normal magnetic field is equal to zero at these symmetrical planes. Hence, the symmetrical planes of the SIW can be considered as a virtual magnetic wall. If the SIW is divided into two halves along the magnetic wall, each half is called half mode substrate integrated waveguide (HMSIW) and it can support nearly half of the original field distribution [**?**], [**?**].

It is also noted that besides the virtual magnetic wall at the center plane along the y-direction, which contributes to the HMSIW design, another symmetrical plane along the center plane in the x-direction exists in the square SIW and in the HMSIW structure, as shown in Fig. **??**. It provides an opportunity to bisect the HMSIW again along the virtual magnetic wall in the x-direction, and each half of the HMSIW is defined as QMSIW in this paper and nearly a quarter of the original field distribution of the SIW structure can be supported.

Fig. **??** shows the configuration of the studied QMSIW,

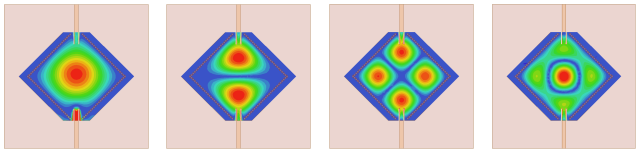

(a) (b) (c) (d)

Fig. 5. Electric field distribution observed at different resonant modes of the square SIW resonator. (a) TM_{11}^{SIW} mode at 2.9 GHz. (b) TM_{12}^{SIW}/TM_{21}^{SIW} mode at 4.56 GHz. (c) TM_{22}^{SIW} mode at 5.8 GHz. (d) TM_{33}^{SIW} mode 6.53 GHz.

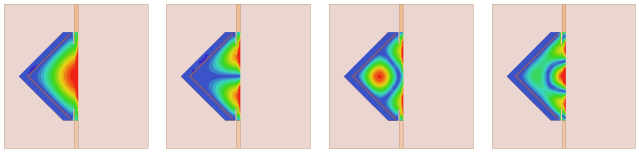

(a) (b) (c) (d)

Fig. 6. Electric field distribution observed at different resonant modes of the HMSIW resonator. (a) The 1st mode at 2.73 GHz. (b) The 2nd mode at 4.38 GHz. (c) The 3rd mode at 5.39 GHz. (d) The 4th mode 6.21 GHz.

which is exactly a quarter of the square SIW. The QMSIW is designed on a Rogers RT3010 substrate with thickness of $h = 1.27$ mm, high dielectric constant ($\epsilon_r = 11.2$) and low loss tangent ($tan\delta = 0.0035$). The via diameter d is 0.6 mm, and the spacing between adjacent vias s is 0.75 mm. The length of the QMSIW legs a is 17 mm.

Fig. **??** shows the comparison of the resonant frequencies between square SIW, HMSIW and QMSIW resonators. The dashed blue curve shows the simulated transmission coefficient of the square SIW resonator shown in Fig. **??**. The predicted resonances for the TM_{11}^{SIW}, TM_{12}^{SIW}/TM_{21}^{SIW}, TM_{22}^{SIW} and TM_{33}^{SIW} modes are excited at 2.9 GHz, 4.56 GHz, 5.8 GHz and 6.53 GHz. The dotted black curve and the solid red curve give the results of the HMSIW and QMSIW resonators, respectively. It should be pointed out that the resonant frequencies of HMSIW and QMSIW resonators are slightly shifted comparing with the corresponding SIW, because of the fringing field of the equivalent magnetic walls. The resonant frequencies for the QMSIW are at 2.6 GHz, 5.12 GHz, and 5.94 GHz, corresponding to TM_{01}/TM_{10}, TM_{02}/TM_{20}, and TM_{12}/TM_{21} modes, respectively. These three kinds of resonant modes are similar to the 1st, the 3rd and the 4th resonant modes in the square SIW and HMSIW resonators. However, the 2nd resonant mode for the square SIW and HMSIW resonators does not appear in the QMSIW resonator. This is because the virtual magnetic walls along the x and y- axis in the square SIW exist for the TM_{11}^{SIW}, TM_{22}^{SIW} and TM_{33}^{SIW} modes, but not for the TM_{12}^{SIW}/TM_{21}^{SIW} mode. This can be seen from the electric field distributions shown in Fig. **??**-**??**.

The electric field distributions of square SIW, HMSIW and QMSIW resonators are studied. Fig. **??** shows electric field distributions of the square SIW resonator at 2.9 GHz, 4.56 GHz, 5.8 GHz and 6.53 GHz corresponding to TM_{11}^{SIW}, TM_{12}^{SIW}/TM_{21}^{SIW}, TM_{22}^{SIW} and TM_{33}^{SIW} modes, respectively. Fig. **??** shows the electric field distributions in the HMSIW resonator at 2.73 GHz, 4.38 GHz, 5.39 GHz and 6.21 GHz, corresponding to the first four resonant modes. The electric field distribution of each mode in HMSIW is quite similar to half of the electric field distribution of the corresponding mode in the square SIW.

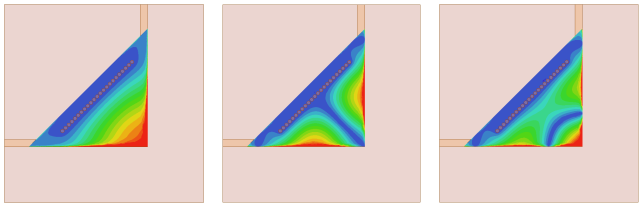

(a) (b) (c)

Fig. 7. Electric field distribution observed at different resonant modes of the QMSIW resonator. (a) TM_{01}/TM_{10} mode at 2.6 GHz. (b) TM_{02}/TM_{20} mode at 5.12 GHz. (c) TM_{12}/TM_{21} mode at 5.94 GHz.

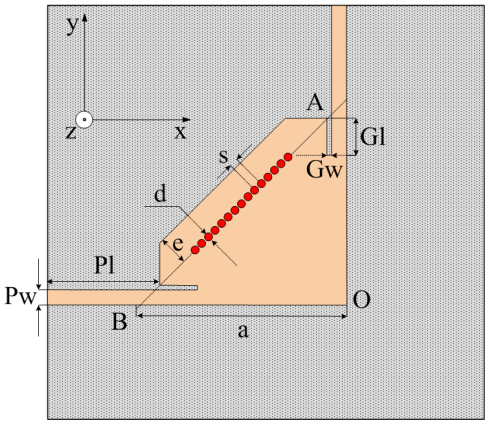

Fig. 8. Layout of the QMSIW filters design based on the proposed isosceles right triangular QMSIW resonator.

The electric field distributions shown in Fig. **??** indicate that the QMSIW resonates at 2.6 GHz, 5.12 GHz, and 5.94 GHz, corresponding to TM_{01}/TM_{10}, TM_{02}/TM_{20}, and TM_{12}/TM_{21} modes, respectively. The resonances are coupled to the interface ports in parallel. It is noted that the virtual magnetic walls at the center plane along the x- and y-directions in the square SIW is only suitable for TM_{11}^{SIW}, TM_{22}^{SIW} and TM_{33}^{SIW} modes, as shown in Fig. **??** and Fig. **??**. However, it is not available for the TM_{12}^{SIW}/TM_{21}^{SIW} mode. It can be seen that the simulated results are the same as the analytical ones shown in Fig. **??**. This is expected and the QMSIW structure simulates the isosceles right triangular waveguide very well.

B. Triple-Mode Filter Design

To demonstrate the application of the proposed triple-mode isosceles right triangular QMSIW resonator, a bandpass filter with a single triangular patch resonator is investigated first. Fig. **??** shows the configuration of the studied QMSIW filter. The QMSIW filter is also designed on Rogers RO3010 substrate with thickness of h = 1.27 mm. The via diameter d is 0.6 mm, and the spacing between adjacent vias is s= 0.75 mm. The condition of $s < 0.25\lambda_g$ should be satisfied to make the array of via holes equivalent to the conventional electric wall [**?**], [**?**], where λ_g is the guided wavelength. The length of the QMSIW legs is 17 mm. The width of the inset microstrip feed is P_w = 1.2 mm and the length

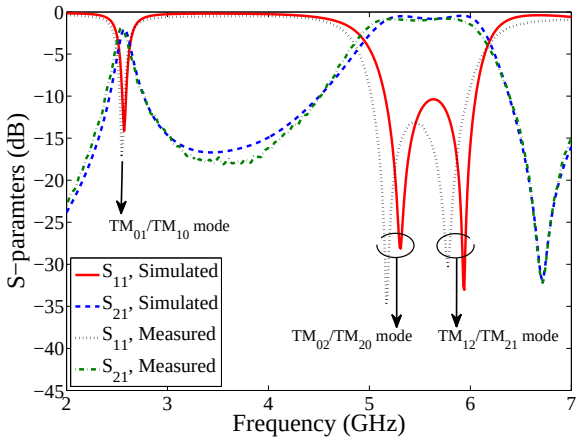

Fig. 9. S-parameters of the QMSIW filter based on the proposed isosceles right triangular QMSIW resonator.

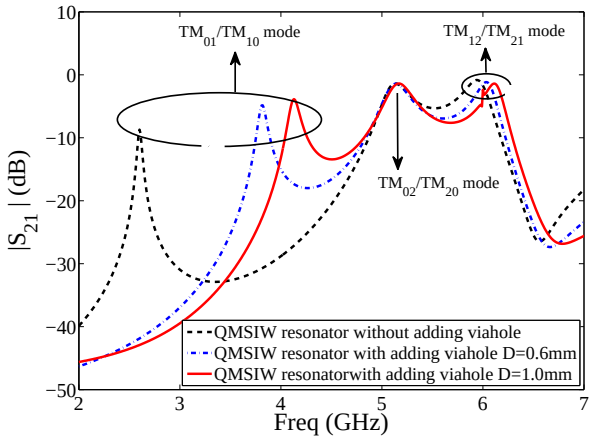

Fig. 11. Simulated transmission coefficients of the QMSIW resonators with an added via hole.

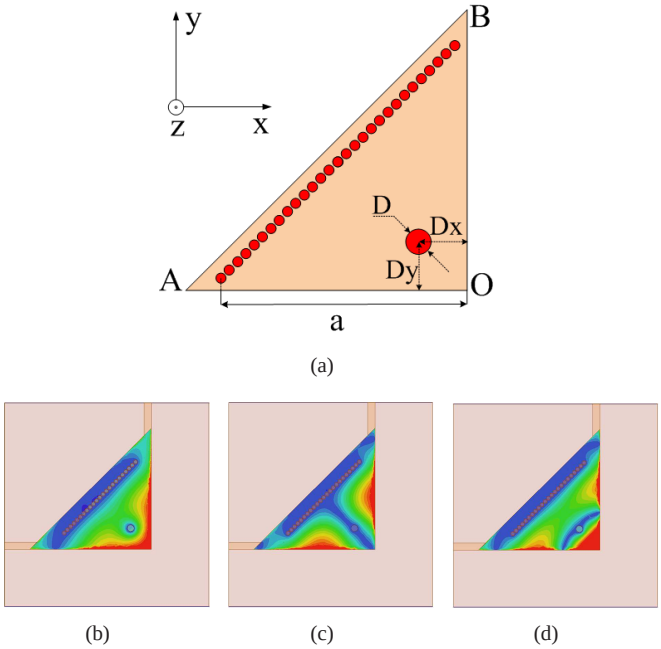

Fig. 10. The configuration and electric field distribution of the QMSIW resonators with an added via hole. (a) The configuration. (b) TM_{01}/TM_{10} mode at 4.13 GHz. (b) TM_{02}/TM_{20} mode at 5.17 GHz. (c) TM_{12}/TM_{21} mode at 6.11 GHz.

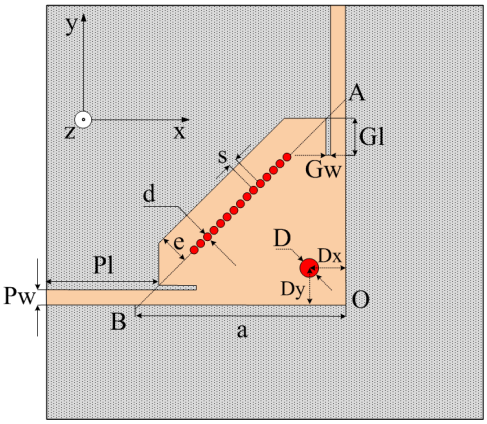

Fig. 12. Layout of the compact triple-mode QMSIW filters based on the proposed isosceles right triangular QMSIW resonator with an added via hole.

is $P_l = 9$ mm. A gap with a width of $G_w = 0.4$ mm and length of $G_l = 3.9$ mm is used. Fifteen via holes are utilized along the hypotenuse of the isosceles right triangular to realize the required electric wall of the QMSIW. Extra copper is added outside the via holes with $e = 2$mm mm to drill the via holes along the hypotenuse of the triangle patch. Simulated and measured reflection coefficients of the designed QMSIW filter are shown in Fig. **??**. The measured results show that the typical TM_{01}/TM_{10} mode resonance occurs at 2.6 GHz, TM_{02}/TM_{20} mode resonance occurs at 5.16 GHz and TM_{12}/TM_{21} mode resonance is obtained at 5.78 GHz.

In order to control the bandwidth and obtain flat insertion loss in the passband, a small via hole is added at the corner of the isosceles right triangular QMSIW resonator, as shown in Fig. **??**. It can shift the TM_{01}/TM_{10} mode resonant frequency effectively, whereas the resonant frequencies of TM_{02}/TM_{20} and TM_{12}/TM_{21} modes will be almost unchanged. Fig. **??**-(d) show the electric field distributions of different resonant modes for the QMSIW resonator with the added via hole. Comparing with electric field distribution of the QMSIW resonator shown in Fig. **??**, it can be found that the added via hole perturbs the electric field distribution for the TM_{01}/TM_{10} mode. However, it does not affect the electric field distributions for the TM_{02}/TM_{20} and TM_{12}/TM_{21} modes, because the added via hole is designed at one particular point, where the electric field of TM_{02}/TM_{20} and TM_{12}/TM_{21} modes is nearly zero.

Fig. **??** plots three sets of simulated frequency responses of the isosceles right triangular QMSIW resonator with different added via holes. The resonant frequencies of TM_{01}/TM_{10} mode increases dramatically, while resonant frequencies for the TM_{02}/TM_{20} and TM_{12}/TM_{21} modes are shifted a little, especially for the TM_{02}/TM_{20} mode. At last, a via hole with diameter of D = 1.0 mm is added at the corner of the QMSIW resonator with $D_x = D_y = 3.4$ mm, and it helps to shift these three resonant frequencies toward the center.

Based on the discussed characteristics of triple resonances

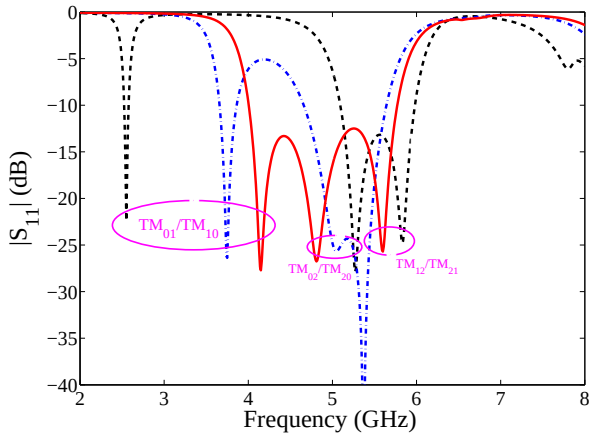

(a)

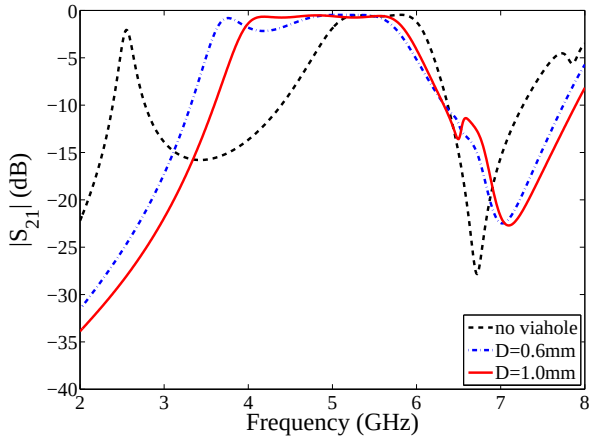

(b)

Fig. 13. S-parameters and group delay of the compact triple-mode QMSIW filter. (a) Reflection coefficients. (b) Transmission coefficients.

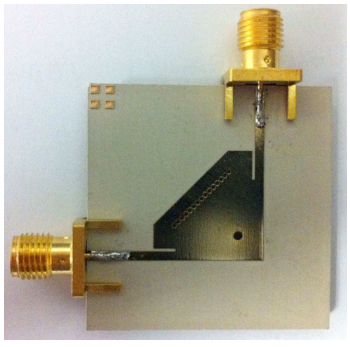

Fig. 14. Prototype of the compact triple-mode QMSIW filters based on the proposed isosceles right triangular QMSIW resonator with an added via hole.

in the isosceles right triangular QMSIW resonator, a compact triple-mode bandpass filter is designed and implemented on the substrate Rogers RO3010. Fig. **??** describes the physical layout of the triple-mode bandpass isosceles right triangular QMSIW filter. The simulated frequency responses of the filters with and without the added via hole around the right corner of the triangular QMSIW is shown in Fig. **??**. It is noted that a triple-mode bandpass filter is realized in a compact structure.

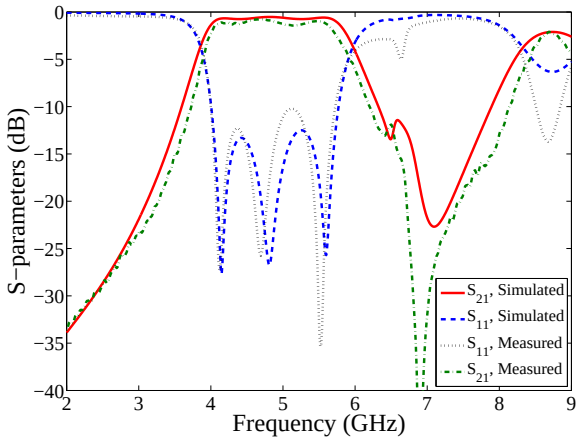

(a)

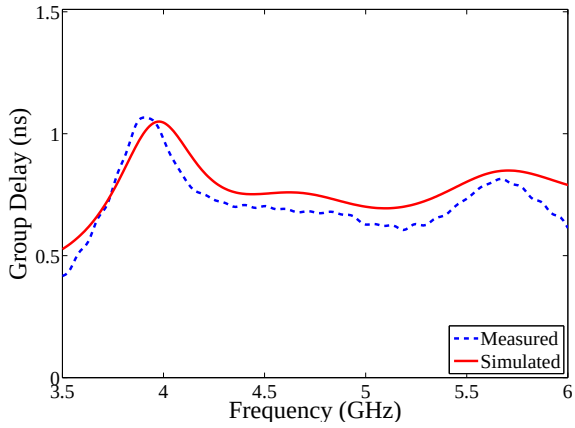

(b)

Fig. 15. S-parameters and group delay of the compact triple-mode QMSIW filter. (a) S-parameters. (b) Group delay.

In order to validate the simulated filtering performance, the compact triple-mode filter designed with isosceles right triangular QMSIW, as shown in Fig. **??**, is fabricated. Fig. **??** shows the photograph of the fabricated filter. Measured results are plotted together with those simulated ones in Fig. **??**, which experimentally verify the attractive wideband filtering performance. The fractional bandwith of the wideband bandpass fitler is 38% at 5.2 GHz, Within the passband the measured return loss is better than 10 dB and the minimum return loss is 10.4 dB at 5.1 GHz. Meanwhile, the measured insertion loss is approximately 0.74 dB at the central frequency of 4.67 GHz. Three transmission poles can be clearly observed at 4.12 GHz, 4.69 GHz and 5.53 GHz in the passband. The group delay of the proposed filter is also measured and shown in Fig. **??**. The group delay is found to be in good agreement with the simulated result over the plotted frequency range. Meanwhile, the in-band group delay for the three-pole bandpass filter is fairly flat in the middle passband, and becomes higher near the lower and upper roll-off edges. The overall passband group delay is less than 1 ns.

It should be pointed out that although the agreement of the measured response with the prescribed frequency responses

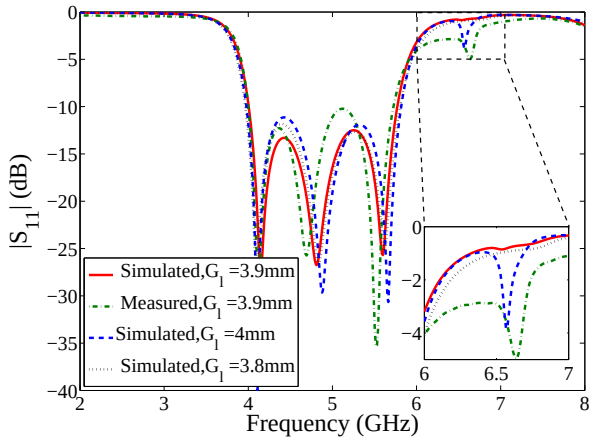

(a)

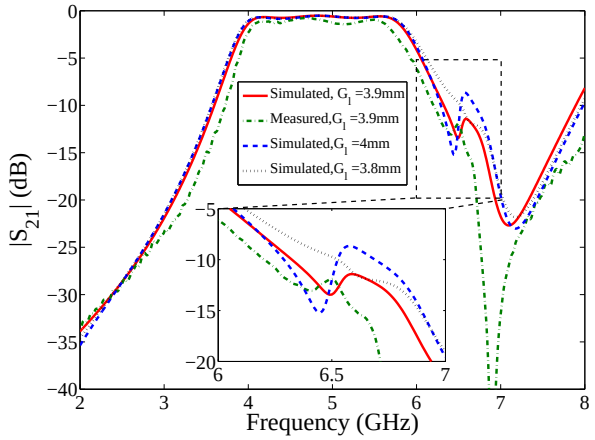

(b)

Fig. 16. Comparison of experimental and full-wave simulated S-parameters of the compact triple-mode QMSIW filter with different G_l as shown in Fig. **??**. (a) Reflection coefficients. (b) Transmission coefficients.

is acceptable, discrepancies are observed and there is a dip in the reflection coefficients at around 6.52 GHz. Considering the simulated frequency responses of the filters with and without the added via hole around the right corner of the triangular QMSIW as shown in Fig. **??**, the dip is not observed. Hence, the added via hole should not contribute to this discrepancy. In this QMSIW structure, the other part requires high quality fabrication is the feeding network. The width of the inset microstrip feed is chosen as $P_w = 1.2$ mm and the length is $P_l = 9$ mm to realize 50 Ω microstrip line, and a gap with a width of $G_w = 0.4$ mm and length of $G_l = 3.9$ mm is used as shown in Fig. **??**. In order to find the cause, a comparison of the frequency responses for the filter with small different dimension of the gap is shown in Fig. **??**. It is noted that a dip appears when the length of the gap is increased slightly. Hence, the dip in the measured reflection coefficient may be attributed to the feeding network and over-etching of the gap in the fabrication process (within the tolerence of the etching machine).

It may be pointed out that our proposed triple-mode filter has some limitations on its bandwidth and the location of the first harmonic in the stopband due to its simple structure and compact size. From the derivations and discussions prsented early, the following design guidelines for our triple-mode filter may be formulated.

- From the design specifications for the triple-mode filter, such as center frequency (f_0) and bandwidth, one can calculate the approximate value for the length of the QMSIW legs a using $a = 1/(f_0\sqrt{\mu\epsilon})$, since the resonant frequency of TM_{02}/TM_{20} mode of QMSIW should be close to the center frequency of the filter.
- Adjust the position of the added via hole around the corner of the QMSIW resonator to shift the resonant frequency of TM_{01}/TM_{10} mode near the lower edge of the passband, while the resonant frequency of TM_{12}/TM_{21} mode should approach the upper edge of the passband.
- Design the feeding network for the filter by varying the gap width and depth.
- Overall optimization of the filter using a full-wave simulator to compensate non-idealities, such as the fringing field of equivalent magnetic walls and the effect of the array of metallic via holes replacing the conventional electric wall.

IV. Conclusion

An isosceles right triangular waveguide with two magnetic walls and one electric wall has been proposed in this paper. The modal solutions of the isosceles right triangular waveguide have been obtained from its corresponding square waveguide. The resonant frequencies and electromagnetic field components have then been derived for a resonator made of a short isosceles right triangular waveguide. After that, QMSIW has been introduced to realize the required boundary conditions. The electric field distributions of the QMSIW have been simulated, which are similar to the theoretically predicted results of the triangular waveguide resonator. Finally, a compact planar triple-mode filter has been designed based on the proposed isosceles right triangular QMSIW. Both simulated and measured results have shown that the proposed isosceles right triangular waveguide resonator or the QMSIW is an attractive and promising candidate to design compact planar triple-mode filters.

References

[1] J. S. Hong and M. Lancaster, *Microstrip Filters for RF/Microwave Applications*. New York: Wiley, 2001.

[2] J. S. Hong and S. Z. Li, "Theory and experiment of dual-mode microstrip triangular patch resonators and filters," *IEEE Trans. Microw. Theory Tech.*, vol. 52, no. 4, pp. 1237–1243, Apr. 2004.

[3] S. Amari and U. Rosenberg, "New in-line dual- and triple-mode cavity filters with nonresonating nodes," *IEEE Trans. Microw. Theory Tech.*, vol. 53, no. 4, pp. 1272–1279, Apr. 2005.

[4] C. Lugo and J. Papapolymerou, "Planar realization of a triple-mode bandpass filter using a multilayer configuration," *IEEE Trans. Microw. Theory Tech.*, vol. 55, no. 2, pp. 296–301, Feb. 2007.

[5] K. Srisathit, A. Worapishet, and W. Surakampontorn, "Design of triple-mode ring resonator for wideband microstrip bandpass filters," *IEEE Trans. Microw. Theory Tech.*, vol. 58, no. 11, pp. 2867–2877, Nov. 2010.

[6] A. Torabi and K. Forooraghi, "Miniature harmonic-suppressed microstrip bandpass filter using a triple-mode stub-loaded resonator and spur lines," *IEEE Microw. and Wireless Compon. Lett.*, vol. 21, no. 5, pp. 255–257, May 2011.

[7] S. Zhang and L. Zhu, "Compact and high-selectivity microstrip bandpass filters using triple-/quad-mode stub-loaded resonators," *IEEE Microw. and Wireless Compon. Lett.*, vol. 21, no. 10, pp. 522–524, Oct. 2011.
[8] J.-K. Xiao and H.-F. Huang, "New microstrip filter using single right-angled triangular patch resonator," in *Microwave, Antenna, Propagation and EMC Technologies for Wireless Communications, IEEE International Symposium on*, 2009, pp. 1167 – 1170.
[9] J. S. Hong, H. Shaman, and Y. H. Chun, "Dual-mode microstrip open-loop resonators and filters," *IEEE Trans. Microw. Theory Tech.*, vol. 55, no. 8, pp. 1764–1770, Aug. 2007.
[10] F. Wei, W. T. Li, X. W. Shi, and Q. L. Huang, "Compact UWB bandpass filter with triple-notched bands using triple-mode stepped impedance resonator," *IEEE Microw. and Wireless Compon. Lett.*, vol. 22, no. 10, pp. 512–514, Oct. 2012.
[11] R. Li, S. Sun, and L. Zhu, "Synthesis design of ultra-wideband bandpass filters with composite series and shunt stubs," *IEEE Trans. Microw. Theory Tech.*, vol. 57, no. 3, pp. 684–692, Mar. 2009.
[12] D. Deslandes and K. Wu, "Single-substrate integration technique of planar circuits and waveguide filters," *IEEE Trans. Microw. Theory Tech.*, vol. 51, no. 2, pp. 593 – 596, Feb. 2003.
[13] Y. L. Zhang, W. Hong, K. Wu, J. X. Chen, and H. J. Tang, "Novel substrate integrated waveguide cavity filter with defected ground structure," *IEEE Trans. Microw. Theory Tech.*, vol. 53, no. 4, pp. 1280–1287, Apr. 2005.
[14] Y. Wang, W. Hong, Y. Dong, B. Liu, H. J. Tang, J. Chen, X. Yin, and K. Wu, "Half mode substrate integrated waveguide (HMSIW) bandpass filter," *IEEE Microw. and Wireless Compon. Lett.*, vol. 17, no. 4, pp. 265 –267, Apr. 2007.
[15] B. Liu, W. Hong, Y.-Q. Wang, Q.-H. Lai, and K. Wu, "Half mode substrate integrated waveguide (HMSIW) 3-dB coupler," *IEEE Microw. and Wireless Compon. Lett.*, vol. 17, no. 1, pp. 22 –24, Jan. 2007.
[16] X. P. Chen, K. Wu, and Z. L. Li, "Dual-band and triple-band substrate integrated waveguide filters with chebyshev and quasi-elliptic responses," *IEEE Trans. Microw. Theory Tech.*, vol. 55, no. 12, pp. 2569–2578, Dec. 2007.
[17] B. Potelon, C. Quendo, J.-F. Favennec, E. Rius, S. Verdeyme, and C. Person, "Design of bandpass filter based on hybrid planar waveguide resonator," *IEEE Trans. Microw. Theory Tech.*, vol. 58, no. 3, pp. 635–644, Mar. 2010.
[18] C. Jin, A. Alphones, and L. C. Ong, "Broadband leaky-wave antenna based on composite right/left handed substrate integrated waveguide," *Electron. Lett.*, vol. 46, no. 24, pp. 1584 –1585, Nov. 2010.
[19] C. Jin and A. Alphones, "Leaky-wave radiation behavior from a double periodic composite right/left handed substrate integrated waveguide," *IEEE Trans. Antennas Propagat.*, vol. 60, no. 4, pp. 1727–1735, Apr. 2012.
[20] K. Gong, W. Hong, Y. Zhang, P. Chen, and C. J. You, "Substrate integrated waveguide quasi-elliptic filters with controllable electric and magnetic mixed coupling," *IEEE Trans. Microw. Theory Tech.*, vol. 60, no. 10, pp. 3071–3078, Oct. 2012.
[21] P. L. Overfelt and D. J. White, "TE and TM modes of some triangular cross-section waveguides using superposition of plane waves," *IEEE Trans. Microw. Theory Tech.*, vol. MTT-34, no. 1, pp. 161–167, Jan. 1986.
[22] H. Uchimura, T. Takenoshita, and M. Fujii, "Development of a "laminated waveguide"," *IEEE Trans. Microw. Theory Tech.*, vol. 46, no. 12, pp. 2348–2443, Dec. 1998.
[23] D. M. Pozar., *Microwave Engineering*. Third Edition, New York: Wiley, 2005.
[24] J. Helszajn and D. S. James, "Planar triangular resonators with magnetic walls," *IEEE Trans. Microwave Theory Tech.*, vol. MTT-26, no. 2, pp. 95–100, Feb. 1978.
[25] F. Xu, K. Wu, and X. Zhang, "Periodic leaky-wave antenna for millimeter wave applications based on substrate integrated waveguide," *IEEE Trans. Antennas Propagat.*, vol. 58, no. 2, pp. 340 –347, Feb. 2010.